PAPER

NJC
www.rsc.org/njc

Time-resolved emission upon two-photon excitation of bis-*N*-carbazolyl-distyrylbenzene: mapping of water molecule distribution in the mouse brain

Evgenia Vaganova,*[a] Shlomo Yitzchaik,*[a] Mark Sigalov,[b] Jan W. Borst,[c] Antonie Visser,[c] Haim Ovadia[d] and Vladimir Khodorkovsky*[be]

[a] *The Inorganic and Analytical Chemistry Department, and The Farkas Center for Light-Induced Processes, The Hebrew University of Jerusalem, Israel. E-mail: gv@cc.huji.ac.il, sy@cc.huji.ac.il; Fax: +972-2-658-5319; Tel: +972-2-658-4199*

[b] *Department of Chemistry, Ben-Gurion University of Negev, Beer-Sheva, Israel. E-mail: msigalov@bgumail.bgu.ac.il; Tel: +972-8-647-9322*

[c] *MicroSpectroscopy Centre, Wageningen University, Wageningen, The Netherlands. E-mail: Ton.Visser@wur.nl, JanWillem.Borst@wur.nl; Fax: +31-(0)317-484801*

[d] *Department of Neurology, The Agnes Ginges Center for Human Neurogenetics, Hadassah University Hospital, Jerusalem, Israel. E-mail: OVADIA@hadassah.org.il; Fax: +972-2-642944*

[e] *Faculté des Sciences de Luminy, Université de la Méditerranée, Marseille, France. E-mail: khodor@luminy.uni-mrs.fr; Fax: +33-4-918-2930*

Received (in St Louis, MO, USA) 3rd December 2004, Accepted 8th June 2005
First published as an Advance Article on the web 7th July 2005

We present a method of mapping the water molecule distribution in mouse brain tissues using injected bis-*N*-carbazolyl-distyrylbenzene and the FLIM technique. The fluorescence lifetime of this two-photon absorbing chromophore diminishes when the amount of water in the surrounding area increases. The fluorescence lifetime of the injected *in vivo* chromophore strongly depends on the content of water in different areas. Thus, lifetimes of 900 ± 50 ps in the hippocampus (extracellular fluid), 520 ± 50 ps in the lateral ventricle (choroid plexus, cerebrospinal fluid), and 400–150 ps in blood vessels were observed. Moreover, the fluorescence lifetime distribution undergoes drastic changes when mice are deprived of water. Statistical analysis of the investigated samples showed that upon water deprivation water content decreased at the border of the hippocampus/lateral ventricle areas and increased in blood vessels.

Introduction

Fluorescence lifetime imaging microscopy (FLIM) is a very useful technique in many areas of bioscience. FLIM allows direct visualization of spatially dependent fluorescence decay,[1–6] whereas fluorescence microscopy imaging primarily shows the localization of species of interest, such as proteins or other macromolecules.[6–11]

Eqn. (1) presents the dependence of the fluorescence intensity on the deactivation time of the excited state[12]

$$I(t) = \sum_{i=1}^{n} \alpha_i e^{-t/\tau_i} \qquad (1)$$

where α_i are the pre-exponential factors (amplitudes), τ_i are the decay times and n is the number of exponential components.

Interactions of the fluorescent molecule in the excited state with neighboring molecules in the ground state are manifested in the spatial distribution of the fluorescence decay. The most important advantage of the FLIM technique is that it does not depend on the chromophore concentration, the excitation intensity and the light path length, conditions that are difficult if possible to control inside biological objects.

The FLIM technique has been shown to be useful for sensing of oxygen,[13] pH,[14–17] calcium,[16,18–19] intracellular sodium,[20] free and protein-bound NADH,[2] macrophage-mediated antigen processing,[21] and glucose.[22,23] The FLIM technique has also been used to study different mechanisms in brain.[24–29] In particular, brain tumor margins were explored by measuring the lifetime of the autofluorescence in brain tissue,[25] release of Zn(II) under electrical stimulation of the mammalian hippocampus was investigated by measuring the fluorescence parameters of injected fluorescent labels[26] and the transport of proteins conjugated with the fluorescent species in elongated tubules of hippocampal neurons was also measured using the fluorescence control.[29]

The scope of the FLIM technique was expanded with the invention of biologically applicable two-photon chromophores. Use of the lower energy wavelengths for excitation decreases the damage to the biological objects, diminishes light scattering and allows deeper penetration into biological tissues. Utilization of ultra-short pulsed lasers (sub-picosecond) solves the problem of protection of biological tissue from radiation damage. Even when the peak power during one pulse is extremely high, the average laser power remains relatively low and not harmful to the biological tissues.

Albota *et al.* have drawn a guideline for the design strategy of two-photon chromophores.[30] It is based on the concept that charge transfer from the ends of a conjugated symmetric molecule towards the center, or *vice versa*, is correlated to

DOI: 10.1039/b418271p

enhanced values of the two-photon absorption cross-section, δ. This concept was tested in a series of bis(styryl)benzene derivatives with D–π–D, D–A–D, and A–D–A structural motifs. Indeed, exceptionally large values of δ were measured, and theoretical predictions and QC calculations attributed this to substantial symmetrical charge redistribution upon excitation.[30]

Recently, we developed a series of two-photon absorbing chromophores involving carbazole moieties as the electron donating groups.[31] Derivatives of this series possess large two-photon cross-section coefficients at ~800 nm, high fluorescence quantum yields and photostability. At the same time, their photochemical behavior strongly depends on the polarity of the solvent. In the present study, bis-*N*-carbazolyl-distyrylbenzene (BND),[31] was chosen as a fluorescent label for the neuroimaging of water molecules in brain tissues.

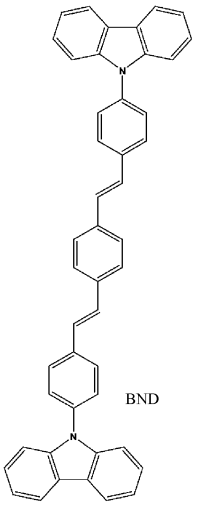

Three kinds of fluids are active in a brain: extracellular, cerebrospinal, and blood. The extracellular fluid compartment includes all water and electrolytes outside of cells (interstitial fluid, plasma, and lymph); cerebrospinal fluid (CSF) mostly contains water, and is formed by ultrafiltration of blood in the choroid plexus (special cells that make up the walls of some collections of arteries in the brain and filter red, white and platelet cells, thus the filtered CSF has no cells, however, ions and glucose are small enough to pass through the filter that makes CSF). CSF circulates through the ventricles as well as flowing around the outside of the brain and through the spinal canal. Hydrostatic pressure and osmotic pressure regulate the movement of water and electrolytes from one part of the ventricle to another. The flow of CSF through the ventricular system of the human brain is a complex phenomenon because of the ventricular system geometry, and it is considered as creep flow due to its low production rate. Apart from cushioning the brain and transporting the biomedical elements, CSF has a major function in buffering extracellular fluids, nutrient supply and participation in brain signaling.[32,33]

Here we demonstrate that the quantitative distribution of water in brain tissues can be visualized by means of injected *in vivo* chromophore and the two-photon FLIM technique.

The brain's self-protection from dehydration is one of the vital biological processes. It was demonstrated that although in the case of dehydration the content of water within several tissues is decreased,[34] the brain water content is maintained.[35] However, the detailed mechanism of brain self-protection from water deprivation is yet unknown.

We investigated the effect of dehydration on the distribution of water molecules at the hippocampus/lateral ventricle area border. Preliminary results presented here show that redistribution of the quantity of water occurs as a result of dehydration and this process can be effectively monitored using BND and the two-photon FLIM technique.

Results and discussion

The chromophore, 4,4′-bis(9-carbazolyl)-distyrylbenzene (BND), was synthesized in 40% yield by the Wittig reaction of *p*-bis(diethylphosphonyl)xylylene and 9-(4-formylphenyl)-carbazole in DMSO in the presence of *t*-BuOK.[31] This derivative possesses a large two-photon absorption cross-section coefficient $\delta_{max} = 1050 \times 10^{-50}$ cm^4 s photon (1050 GM) at 800 nm, high fluorescence quantum yield and photostability.[36]

Fluorescent properties of BND

BND exhibits a broad emission band with the maximum intensity at 454 nm when excited at 378 nm (the quantum yield is 0.68 in 10^{-5} M acetonitrile solution). Similar results were also obtained for 10^{-4} M toluene solution previously.[31,36]

The two-photon fluorescence lifetime imaging for BND solution and its evaluation are shown in Fig. 1. In a typical experiment, a glass slide was covered with a thin layer of the BND solution in acetonitrile. The fluorescence of BND was recorded upon excitation at 800 nm (Fig. 1a). Fig. 1d presents the fluorescence decay and fit to the decay at the cross point (inside the dashed circle, Fig. 1b). With a good approximation ($\chi_r^2 = 1.08$), the fluorescence decay follows the two-exponential decay with a measured fluorescence lifetime of 1161.79 ps.

Evaluation of the statistical assessment of the spatial distribution of the fluorescence lifetime values (Fig. 1c) within the observed area (500 mcm × 540 mcm) is shown in Fig. 1d. A random spatial distribution of the fluorescence lifetime values follows the Poisson distribution.

A comparatively narrow FWHM (full width at half of the maximum) of the statistical distribution, namely 60 ps, indicated that BND possesses high homogeneity of fluorescence decay and does not form aggregates.

Upon excitation at 380 nm in acetonitrile, the fluorescence lifetime was 1170 ps; addition of water caused quenching of BND emission and shortening of the fluorescence lifetime. The most pronounced fluorescence lifetime decrease was observed within the range of the acetonitrile/water molar ratio of 0.6–0.4. Within this range, the BND fluorescence lifetime underwent considerable reduction from 1120 ps to 650 ps. Below the molar ratio of 0.4, further quenching of the fluorescence made measurements difficult.

Fig. 2 illustrates the BND emission quenching caused by addition of water. At the same concentration of BND in solution (confirmed by the absorption spectra), the intensity of the fluorescence drops down by more than 20 times when water is present.

The typical results of the lifetime measurements under different conditions are shown in Fig. 3: (1) the instrument response to the duration of the LED pulse (380 nm); (2) decay of the fluorescence lifetime of BND dissolved in acetonitrile–water with addition of hydrochloric acid, the measured lifetime was 480 ps; (3) in acetonitrile–water solution with molar ratio of 0.48, the measured lifetime was 980 ps; (4) in acetonitrile, the measured lifetime was 1170 ps.

According to the ^{1}H-NMR spectra, BND exists as the *E*,*E* isomer in methylene chloride and acetonitrile solutions. The corresponding *E*,*Z* and *Z*,*Z* isomers are considerably less stable than the *E*,*E* isomer (by 4.4 and 8.4 kcal mol^{-1}, respectively, for the PM3 optimized structures). We assume that stabilization of the less stable isomers involving hydrogen bond formation occurs in the presence of water. Experiments in the presence of various amounts of acids indirectly confirm this assumption. Detailed mechanistic studies are currently under way.

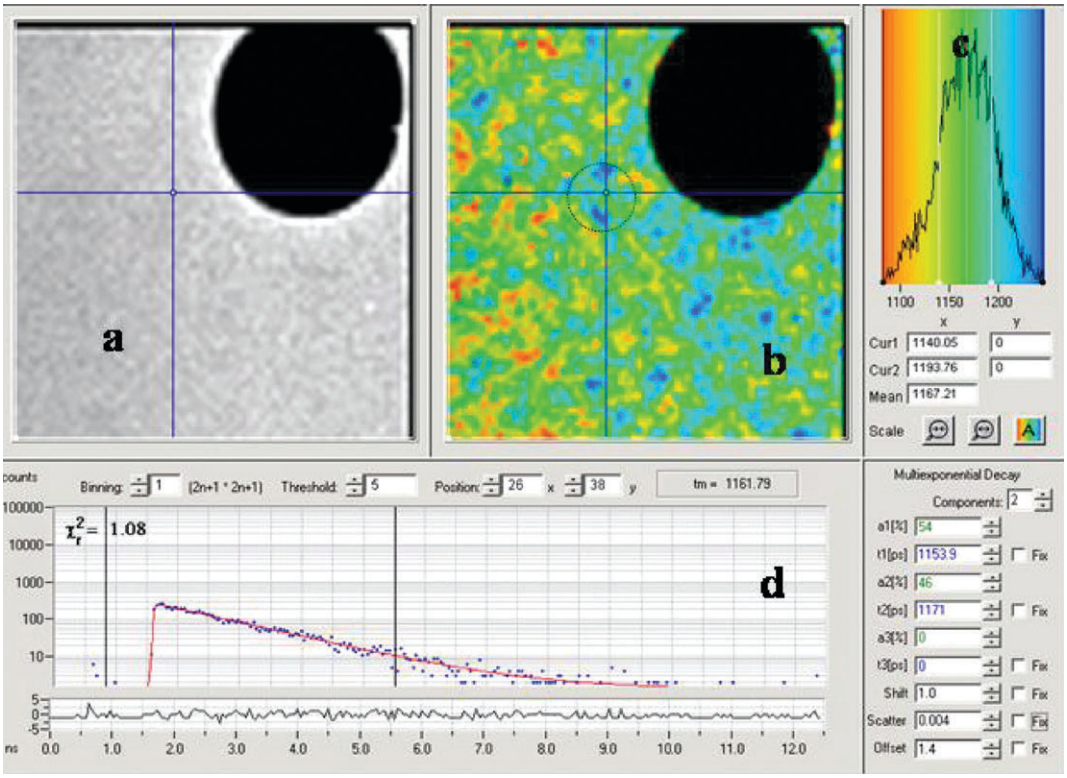

Fig. 1 Imaging of the BND two-photon fluorescence lifetime. The fluorescence was observed at 454 nm upon excitation at 800 nm. (a) Two-photon fluorescence image of a thin layer of the acetonitrile solution (the black spot is a bubble of air in the layer); (b) lifetime imaging of the two-photon fluorescence; (c) the statistical fluorescence lifetime distribution and the color scale of the fluorescence lifetime values; (d) the fluorescence decay (at the cross-marked point in the circle of b) and the fit to the decay.

Fluorescence lifetime imaging of BND injected in the hippocampus

Typical fluorescence lifetime imaging of the investigated areas, lateral ventricle (1) and hippocampus (2), with BND injected *in vivo* into the hippocampus, is shown in Fig. 4. The areas with different fluorescence lifetimes (and, consequently, with different water contents) are mapped as follows: green colored—a lifetime of 520 ± 50 ps—the lateral ventricle area (1); blue colored—a lifetime of 900 ± 50 ps—the hippocampus area (2); yellow-colored—a lifetime of 400–250 ps—the blood vessels (both areas).

Comparison of the FLIM of the hippocampus area filled with the extracellular fluid and the lateral ventricle area with the choroid plexus filled with the cerebrospinal fluid, demonstrates that the changes in the fluorescence lifetime of the chromophore do indeed reflect the amount of water present in each area.

We employed this phenomenon to investigate the effect of water deprivation in the mouse brain in the same area of the lateral ventricle/hippocampus.

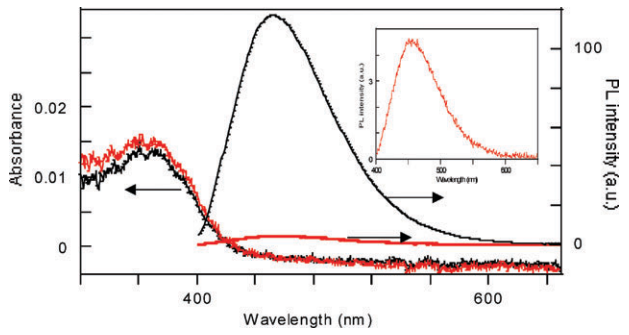

Fig. 2 The absorption (left axis) and emission (right axis) spectra of BND dissolved in acetonitrile (black curve) and acetonitrile–water solution (1 : 1 molar ratio) at a concentration of 10^{-7} M.

Fig. 5 presents a typical fluorescence lifetime image of BND at the boundary of the hippocampus/lateral ventricle areas under normal drinking conditions (a) and under water deprived conditions (b) (the area of the hippocampus where layers of neuronal sheets are present is omitted).

Fluorescence lifetimes of 900.0 ± 25 ps were measured in the hippocampus area under normal conditions (Fig. 5a1), meaning a comparatively narrow range of the fluorescence lifetime distribution. Shortening of the fluorescence lifetime with a much broader statistical distribution of the values (410 ± 100 ps) was observed at the boundary of the lateral ventricle/hippocampus area (Fig. 5a2), indicating the presence of a larger amounts of water.

Parallel experiments using the brain of dehydrated mice produced completely different results. Fig. 5b2 shows the fluorescence lifetime imaging of BND in the same areas. In the hippocampus area the values of the BND fluorescence lifetimes were close to those of the normal conditions: 850.0 ±

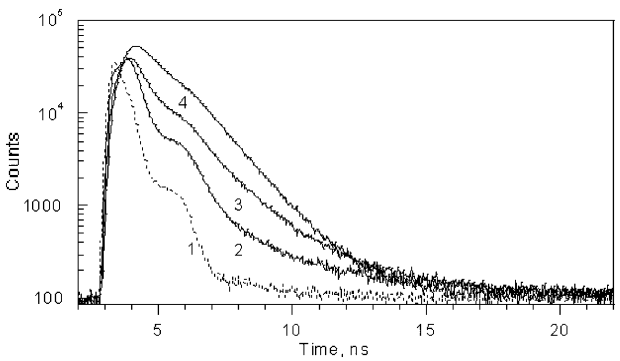

Fig. 3 The fluorescence decay: (1) the instrument response on the LED pulse (λ_{ex} = 380 nm); (2) BND emission λ_{em} = 476 nm (in acetonitrile–water with addition hydrochloric acid); (3) BND emission λ_{em} = 454 nm (in acetonitrile–water solution—molar ratio 0.48); (4) BND emission λ_{em} = 454 nm (in acetonitrile), at room temperature.

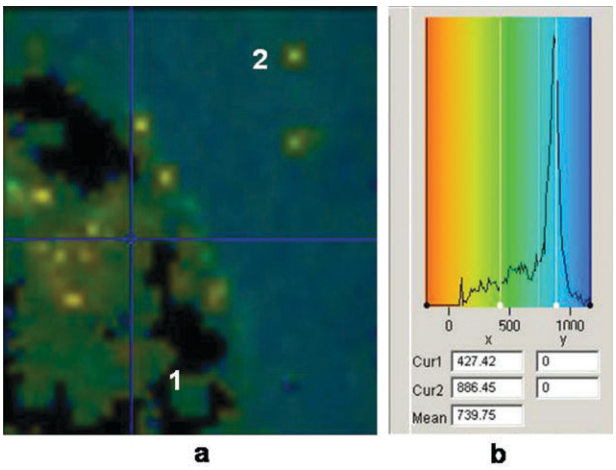

Fig. 4 The typical BND fluorescence lifetime distribution in the lateral ventricle (1) and hippocampus (2) areas; (a) FLIM picture; (b) the statistical distribution and color scale of the fluorescence lifetime.

80 ps *vs.* 900.0 ± 25 ps respectively. However, a significant increase in the BND fluorescence lifetimes of up to 950 ± 100 ps was detected at the boundary (Fig. 5b2) (410 ± 100 ps for the normal conditions). It is noteworthy that the fluorescence lifetime in the blood vessels decreased down to 300–150 ps for the water deprived conditions, meaning an increase in the amount of water in blood.

We also investigated the autofluorescence of the tissues from mice under normal and deprived drinking conditions and the same experiments were done after injection of acetonitrile only. The autofluorescence of the tissue was on the threshold of detection ability under excitation at 800 nm. The same result was obtained in the control cases, when only acetonitrile was injected.

Additionally, we studied the brain samples using a polarized optical microscope. Polarized microscope imaging in the case of water deprivation displayed the tissue at the lateral ventricle/hippocampus boundary as the matter with the enhanced optical activity, meaning formation of a structure with increased optical anisotropic properties. Structures with increased optical anisotropic properties can be result of the decreasing water content.

To summarize, we demonstrated shortening of the BND fluorescence lifetime as a result of BND interaction with water. The FLIM technique applied along with BND can be used to map water distribution in biological tissues.

Apparently, water deprivation leads to a decrease in the content of water in the area of lateral ventricle/hippocampus boundary.

Conclusion

Interaction of BND with water upon irradiation leads to quenching of fluorescence and diminishing fluorescence lifetime. The mechanism of this interaction is currently under investigation. The high sensitivity of the photochemical behavior of BND to the amount of water present allows effective mapping of biological tissues demonstrated in the present study by imaging of the mouse brain using the FLIM technique.

Experimental

Bis-*N*-carbazolyl-distyryl benzene (BND) was injected in the hippocampus area of two groups of mice. Mice: female C57Bl mice (20 g) (Harlan) were kept in pathogen free conditions and given water and food *ad libitum*.

In each group, half the animals were subjected to conditions of water deprivation 12 h prior to use. The other group had free access to water.

Mice were anesthetized with sodium pentobarbital (3 mg per 100 g body weight; intraperitoneally) and placed under a stereotaxic apparatus (Kopf Instruments). The site of injection was chosen according to a mouse brain atlas and coordinates of the hippocampus. Test materials (2 μl) were injected into the hippocampus using a microsyringe inserted through a bore hole in the skull. Mice were sacrificed after 15 min and the brain was excised. Frozen sections (10 μm) were analyzed for fluorescence.

FLIM was performed using a Biorad Radiance 2100 MP system in combination with a Nikon TE 300 inverted microscope. Two-photon excitation pulses were generated by a Ti:Sapphire laser (Coherent Mira) that was pumped by a 5 W Coherent Verdi laser. Pulse trains of 76 MHz (150 fs pulse duration, 800 nm center wavelength) were produced. The excitation light was directly coupled into the microscope and focused onto the sample using a CFI Plan Apochromat 20 × (N.A. 0.75). Fluorescent light was detected using non-descanned single photon counting detection, which is the most sensitive solution for two-photon imaging. For the FLIM experiment the Hamamatsu R3809U MCP PMT was used, which has a typical time resolution of around 50 ps. Bis-*N*-carbazolyl-distyrylbenzene (BND) emission was selected using a 450DF80 nm band-pass filter. Images with a frame size of

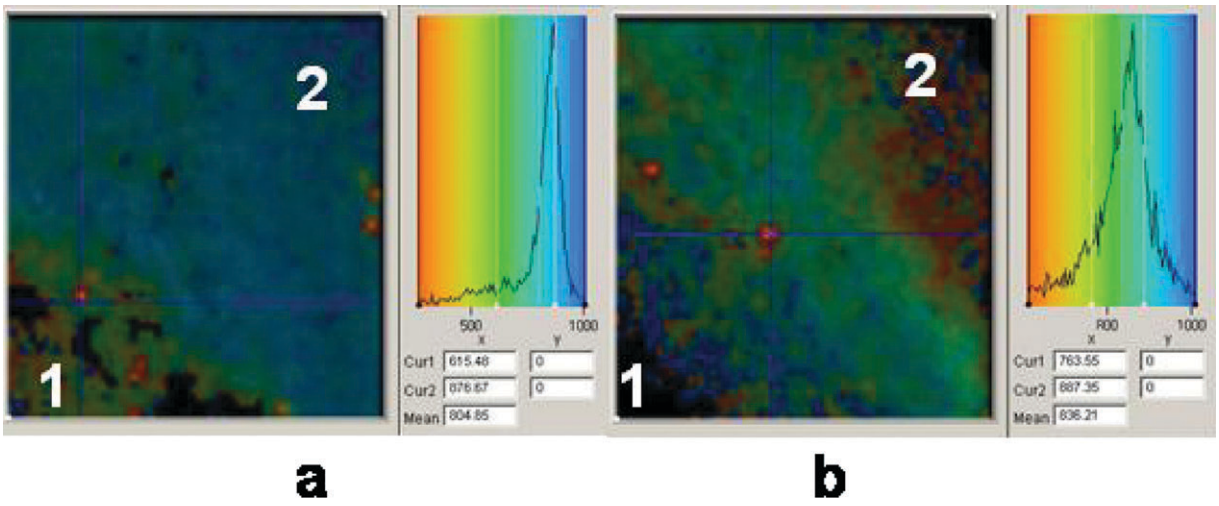

Fig. 5 The typical fluorescence lifetime distribution of BND at the boundary of the hippocampus (1) and lateral ventricle (2) areas; (a) normal water drinking; (b) water deprivation.

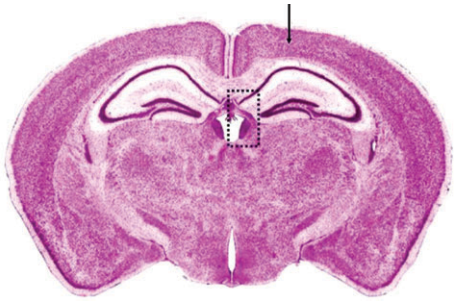

Fig. 6 Scheme of the injection place and the fluorescence lifetime observations (dotted rectangle).

64 × 64 pixels were acquired using the Becker and Hickl SPC 830 module.[37] The average count rate was 2.10^4 photons s^{-1}, for an acquisition time of 90 s. From the intensity images obtained, complete fluorescence lifetime decays were calculated per pixel and fitted using a double exponential decay model.

Fluorescence lifetime measurements were done on BND solution in acetonitrile (10^{-5} M); acetonitrile–water with different molar ratios—acetonitrile–water, BND concentration 10^{-5} M; acetonitrile–water with addition of hydrochloric acid (3×10^{-5} M). Measurements were made by means of FluoTime 200 (PicoQuant GmbH) with a pulsed diode laser PDL 800 – B, $\lambda = 380$ nm, pulse FWHM 54 ps, repetition frequency 20 MHz, maximum power 0.73 mW, with Data Analysis Software FluoFit (PicoQuant GmbH). For pulse control a solution of Ludox was used. The solutions were purged with a flow of argon prior to observation for oxygen elimination.

Excitation and PL spectra were taken on a Shimadzu RF-5301PC spectrofluorimeter. Samples were placed into a 3.5 mm optical path quartz cuvette, and data were collected at right angles to the excitation beam.

The polarized optical microscope images were taken with a microscope Axioskop 2 plus (Zeiss), with available transmitted-light polarization technique.

The scheme of the experiments is presented in Fig. 6. The black arrow points to the site of the chromophore injection and the dashed black line marked rectangle shows the place of the observation, the hippocampus/lateral ventricle area. Brains were excised and immersed in liquid nitrogen. Coronal slices were made at the medial hippocampus.

The samples were stored in liquid nitrogen, and then in dry ice during several days transportation. No preservatives were used for the samples' protection.

Acknowledgements

We gratefully acknowledge financial support from the Israel Ministry for Immigrant Absorption. Fruitful discussions with Dr L. Shapiro and the technical assistance of Mrs. A. Itzik and E. Reinharz are greatly appreciated.

References

1 J. R. Lakowicz, H. Szmacinski, K. Nowaczyk and M. L. Johnson, *Proc. Natl. Acad. Sci. USA*, 1992, **89**, 1271–1275.
2 P. I. H. Bastiaens and A. Squire, *Trends Cell Biol.*, 1999, **9**, 48–52.
3 M. Elangovan, R. N. Day and A. Periasamy, *J. Microsc. (Oxford)*, 2002, **205**, 3–14.
4 W. Becker, A. Bergmann, J. W. Borst, M. A. Hink and A. J. W. G. Visser, *Biophys. J.*, 2003, **84**, 313A–313A.
5 Y. Chen, J. D. Mills and A. Periasamy, *Differentiation*, 2003, **71**, 528–541.
6 B. Valeur, *Molecular Fluorescence, Principles and Applications*, Wiley-VCH, Weinheim, 2001.
7 *Fluorescence Microscopy of Living Cells in Culture, Part A*, ed. D. L. Taylor, Academic, New York, 1989.
8 *Fluorescence Microscopy of Living Cells in Culture, Part B*, ed. D. L. Taylor and Y. Wang, Academic, New York, 1989.
9 *Confocal Microscopy*, ed. T. Wilson, Academic, New York, 1997.
10 C. J. Daly and J. C. McGrath, *Pharmacol. Ther.*, 2003, **100**, 101–118.
11 R. M. Hoffman, *Acta Histochem.*, 2004, **106**, 77–87.
12 G. G. Guilbault, *Practical Fluorescence, Theory, Methods and Techniques*, Marcel Dekker Inc., New York, 1990, p. 583.
13 J. R. Lakowicz and G. Weber, *Biochemistry*, 1973, **12**, 4161–4170.
14 J. R. Laws and L. Brand, *J. Phys. Chem.*, 1979, **83**, 795–802.
15 A. Gafni and L. Brand, *Chem. Phys. Lett.*, 1978, **58**, 346–350.
16 J. R. Lakowitcz and H. Szmacinski, *Sens. Actuators, B*, 1993, **11**, 133–143.
17 H.-J. Lin, P. Herman, J. S. Kang and J. R. Lakowicz, *Anal. Biochem.*, 2001, **294**, 118–125.
18 S. M. Keating and T. G. Wensel, *Biophys. J.*, 1991, **59**, 186–202.
19 M. Hof, G. R. Fleming and V. Fidler, *Proteins—Structure Function and Genetics*, 1996, **24**, 485–494.
20 H. Szmacinski and J. R. Lakowicz, *Anal. Biochem.*, 1997, **250**, 131–138.
21 T. French, P. T. C. So, D. J. Weaver, T. Coelhosampaio, E. Gratton, E. W. Voss and J. Carrero, *J. Microsc. (Oxford)*, 1997, **185**, 339–353.
22 L. Tolosa, H. Szmacinski, G. Rao and J. R. Lakowicz, *Anal. Biochem.*, 1997, **250**, 102–108.
23 N. DiCesare and J. R. Lakowicz, *Anal. Biochem.*, 2001, **294**, 154–160.
24 J. C. Augustinack, J. L. Sanders, L. H. Tsai and B. T. Hyman, *J. Neuropathol. Exp. Neurol.*, 2002, **61**, 557–564.
25 L. Marcu, J. A. Jo, P. V. Butte, W. H. Young, B. K. Pikul, K. L. Black and R. C. Thompson, *Photochem. Photobiol.*, 2004, **80**, 98–103.
26 R. B. Thompson, W. O. Whetsell, Jr., B. P. Maliwal, C. A. Fierke and C. J. Frederickson, *J. Neurosci. Methods*, 2000, **96**, 35–45.
27 R. B. Thompson, D. Peterson, W. Mahoney, M. Cramer, B. P. Maliwal, S. W. Suh, C. Frederickson, C. Fierke and P. Herman, *J. Neuroscience Method.*, 2002, **118**, 63–75.
28 M. Nishi, M. Tanaka, K. Matsuda, M. Sunaguchi and M. Kawata, *J. Neurosci.*, 2004, **24**, 4918–4927.
29 C. Kaether, P. Skehel and C. G. Dotti, *Mol. Biol. Cell*, 2000, **11**, 1213–1224.
30 M. Albota, D. Beljonne, J. L. Bredas, J. E. Ehrlich, J. Y. Fu, A. A. Heikal, S. E. Hess, T. Kogej, M. D. Levin, S. Marder, D. McCordMaughon, J. W. Perry, H. Röckel, M. Rumi, G. Subramaniam, W. W. Webb, X. L. Wu and C. Xu, *Science*, 1998, **281**, 1653–1657.
31 M. Sigalov, A. Ben-Asuly, L. Shapiro, A. Ellern and V. Khodorkovsky, *Tetrahedron Lett.*, 2000, **41**, 8573–8576.
32 A. Van Harreveld, *Brain Tissue Electrolytes*, Butterworths, London, 1966.
33 *The Blood-Brain Barrier, Cellular and Molecular Biology*, ed. W. M. Pardridge, Raven Press, New York, 1993.
34 R. K. Reed and H. Wiig, *Acta Physiol. Scand.*, 1981, **113**, 297–305.
35 R. Duelli, M. H. Maurer, S. Heiland, V. Elste and W. Kuschinsky, *Neurosci. Lett.*, 1999, **271**, 13–16.
36 Z. Kotler, J. Segal, M. Sigalov, A. Ben-Asuly and V. Khodorkovsky, *Synth. Met.*, 2000, **115**, 269–273.
37 M. A. Hink, J. W. Borst and A. J. W. G. Visser, *Biophotonics, Part B Methods in Enzymology*, Academic Press, New York, 2003, vol. 361, pp. 93–112.